JOURNAL OF APPLIED POLYMER SCIENCE VOL. 13, PP. 1083–1111 (1969)

Influence of Water on Stress Corrosion Cracking of Epoxy Bonds

SHELDON MOSTOVOY and E. J. RIPLING, *Materials Research Laboratory, Inc., Glenwood, Illinois 60425*

Synopsis

Environment assisted fracturing, or stress corrosion cracking of adhesive joints in liquid water or a humid atmosphere was shown to occur at values of applied crack extension force $\mathcal{G}_a$ considerably below those required for onset of opening-mode rapid fracture $\mathcal{G}_c$. The minimum value of $\mathcal{G}_a$ below which no cracking was observed, $\mathcal{G}_{scc}$, was dependent on the relative humidity and the particular adhesive used. For two adhesive systems, the one with the lower hardener content and post cure temperature showed both a lower absolute value of $\mathcal{G}_{scc}$ and a lower ratio of $\mathcal{G}_{scc}$ to $\mathcal{G}_c$. The value of $\mathcal{G}_{scc}$ for both adhesive systems decreased as the humidity was increased. As the relative humidity approached 100%, the value of $\mathcal{G}_{scc}$ approached its value for liquid water. Values of $\mathcal{G}_c$ for the two adhesives differed by a ratio of approximately 2:1. When water was introduced to the crack tip, $\mathcal{G}_c$ for the less tough material increased while it was not significantly changed for the tougher material.

Fracturing occurs in structural adhesive joints, and other brittle materials by the extension of some initially present crack-like flaw. The crack may extend at rates as slow as mils per minute or as high as thousands of feet per minute. The techniques of fracture mechanics are useful in describing crack extension over the range of these extremes.

Early applications of fracture mechanics were concerned with the onset of rapid fracture of an initially stationary flaw when an opening mode load (i.e. one whose direction is normal to the crack surface) became critical. This load at instability, the flaw size, and a factor determined by the structure or specimen geometry define the fracture toughness of the material, a property which can be expressed either in terms of a stress field or an energy parameter. The former definition of opening mode fracture toughness, the critical stress intensity factor, designated K_{Ic}, has the units of ksi-in$^{1/2}$ (in the British system). The units of the critical strain energy release rate $\mathcal{G}_c$ are in.-lb/in.^{2}, or (in the metric system) ergs/cm^2; where 1 in.-lb/in.^{2} equals 1.75×10^5 erg/cm.^{2} Since these can be reduced to units of lb/in. or dyne/cm. $\mathcal{G}_c$ is also referred to as the crack extension force. Inferentially, the force is per unit length of the leading edge of the crack. The subscript I which describes opening mode loading has also been used to denote that the conditions satisfy those for plane strain. Since opening mode loading was used throughout this study and the conditions for plane strain were

always met, the subscript I is omitted, and the critical strain energy release rate for the onset of rapid fracture is designated as $\mathcal{G}_c$.

In addition to the high unstable rates of crack propagation which occur at $\mathcal{G}_c$, the cracking rate $\dot{a}$ can also be a function of the applied crack extension force. For such driven cracks, the symbol for toughness is $\mathcal{G}(\dot{a})$.

In the presence of an aggressive environment, $\mathcal{G}(\dot{a})$ is greatly reduced. A complete description of slow crack growth requires two types of information for the environment of interest. The first is the value of $\mathcal{G}_a$ below which no crack propagation occurs. This quantity, which depends on the environment is designated $\mathcal{G}_{scc}$, and, like $\mathcal{G}_c$, is thought to be material property. The second is the $\dot{a}$ dependence of $\mathcal{G}(\dot{a})$ for values of $\mathcal{G}_a$ above $\mathcal{G}_{scc}$. Both of these as well as the crack morphology for stress corrosion cracking, are discussed in this study. The epoxy system used is the same as the one whose rapid cracking behavior under the influence of increasing load was previously reported.[1]

BACKGROUND ON FRACTURE TOUGHNESS OF THE ADHESIVE SYSTEM

In the earlier paper[1] the authors described the fracture toughness of an adhesive system consisting of Dow epoxy resin (DER) 332 and the room temperature curing amine hardener, TEPA, with aluminum adherends. The influence of ratio of resin to hardener and post-cure temperature on fracture toughness was evaluated, and the toughness of the adhesive was

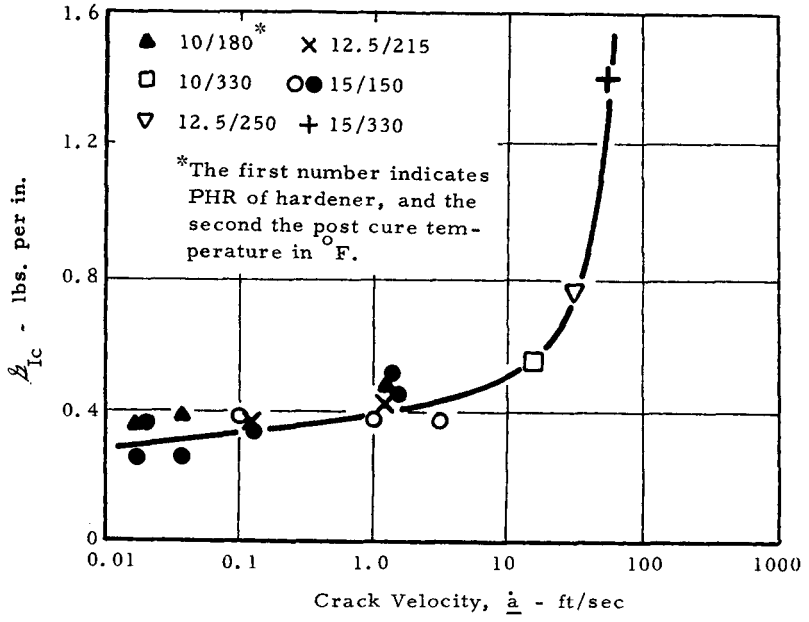

Fig. 1. Dependence of toughness on crack velocity.

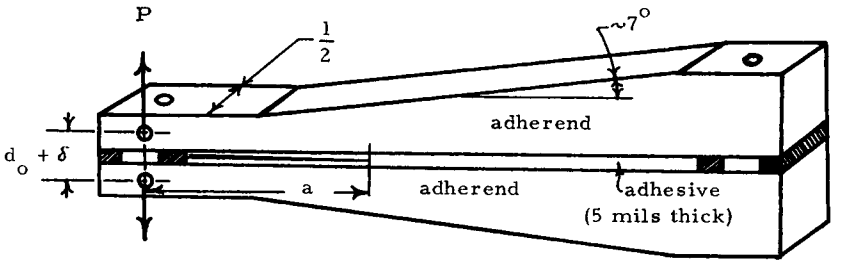

Fig. 2. Contoured double cantilever beam adhesive specimen (m = 90). Specimen is contoured, in accordance with the m value, which is approximated by a 7° half-angle.

found to increase with both hardener content and post-cure temperature. By varying the combination of composition and heat-treatment, the toughness was found to vary by a factor of 4:1.

Not only the toughness, but also the crack velocity varied as a function of these two variables: cracking was observed at 10–100 ft/sec for those combinations of composition and post-cure temperature that resulted in high toughness, and at velocities less than 10 ft/sec for the less tough materials (Fig. 1).

The testing technique used for collecting these data was also described in detail earlier.[2,3] As pointed out in these previous papers, the specimen whose dimensions are shown in Figure 2 has the characteristic that the crack extension force is proportional to the square of the applied load P and independent of crack length a. When making an increasing load test with such a specimen, P is generally plotted as a function of its displacement δ, as shown in Figure 3. If crack extension is produced by a condition of constant displacement for this crack-line loaded specimen, the crack is self-arresting. Hence, the specimen can be loaded until some crack extension occurs, unloaded, reloaded, etc., in order to collect a number of data points on a single specimen. The heavy straight lines in Figure 3 labeled b, c, and d are unloading and reloading curves obtained when the crack was stationary between interrupted extensions.

When such P–δ curves are made on specimens whose properties are shown on the horizontal and vertical branch of the curve in Figure 1, two completely different types of behavior are found. On the horizontal branch cracking occurs at a velocity that is a direct reflection of the rate at which the test machine crosshead is moving. Typical curves of this type are shown in Figure 3a, and because the load and $\mathcal{G}(\dot{a})$ remains constant while the crack extends, the curves are designated as flat.

The adhesive specimens whose properties are shown in the vertical branch of Figure 1, crack at a rate that is limited by material or adhesive joint properties rather than by crosshead speed. In this case, when the load is increased to its critical value, the crack accelerates rapidly to a very high velocity and then decelerates comparatively slowly to the velocity as-

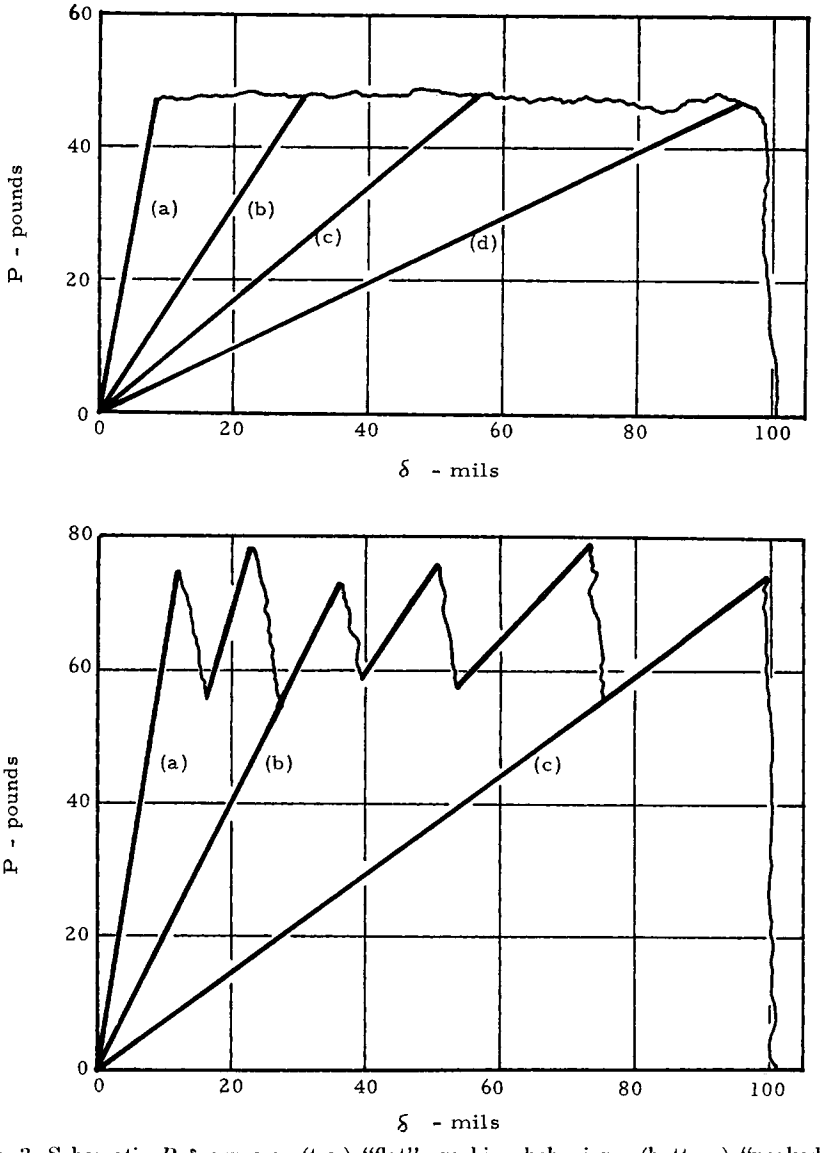

Fig. 3. Schematic P–δ curves: (top) "flat" cracking behavior; (bottom) "peaked" cracking behavior.

sociated with its arrest. The P–δ curve in this case displays two points of instability: one at which the crack begins to run and a second where it stops (Fig. 3*b*). This type of curve is referred to as peaked. The upper critical load is associated with the fracture toughness for crack initiation, and the lower one with fracture toughness for crack arrest.

This difference in crack velocity for the flat and peaked P–δ curve materials is not apparent in fracture morphology. Although the tougher ad-

hesives, that show peaked curves, form rougher fracture surfaces than the less tough material, particularly on a fine scale, both fractures travel essentially in the center of the bond (CoB fracture), leaving an approximately equal amount of adhesive on the two separated adherend surfaces. Indeed, only when a large excess of hardener is used will the separation remain near one or the other interface (IF) under the action of a continuously increasing load.

EXPERIMENTAL

Specimen Type and Manufacturing Procedure

Except for the time-lapse cinematographic study, where glass adherends were used, the aluminum alloy 2024-T351 was used exclusively for the adherends in this study. Half-specimens were machined such that a linear compliance specimen was obtained after bonding. This specimen shape, shown in Figure 2, has been described previously.[2,3] The specimen shape has the advantage that the value of the stress intensity factor K or strain energy release rate $\mathcal{G}$ is independent of crack length.

Preparation of the aluminum adherends prior to bonding has also been described.[2,3] Briefly, this consists of sawing and milling blanks to a standard shape and then cleaning, using a standard solution commonly used to prepare aluminum for bonding with epoxy adhesives. Once cleaned, rinsed and dried, the adherends are bolted together separated by 0.005-in. shims. This assembly is then Teflon-taped to provide a casting dam for the epoxy and to avoid filling the loading holes or covering other parts of the adherend with the adhesive overrun. Five of the taped adherend assemblies are then placed on a large rectangular hot plate and heated to 150° F. Epoxy resin (DER 332) heated to 110°F is then mixed with room temperature hardener (tetraethylenepentamine, TEPA) and stirred until the cloudy solution first obtained when the two components are mixed, disappears. The fluid, thoroughly mixed, adhesive is poured into the bond cavity starting from one end. Due to its fluidity the small liquid pool flows into the 5-mil separation from the one edge displacing the air without entrapment of bubbles. This liquid pool is continuously replenished from the supply beaker as the liquid fills the cavity and flows along the taped-off area. Each specimen on the hot plate is poured in this way and once pouring is completed the excess epoxy is removed by drawing a glass rod over the taped area. This causes all but a thin layer of the adhesive to be removed from the exposed adherends at the bonding cavity, as shown schematically in Figure 4.

After the pouring operation the hot plate is turned off and the specimens are allowed to cool slowly. During this period gelation occurs and after about an hour the specimens can be handled. At this point the tape is removed and the specimen placed in an air circulating oven for a 5-hr post cure. Once post-cured, the specimen is ready for testing. The condition of the adhesive, i.e., its composition and post cure temperature, are recorded

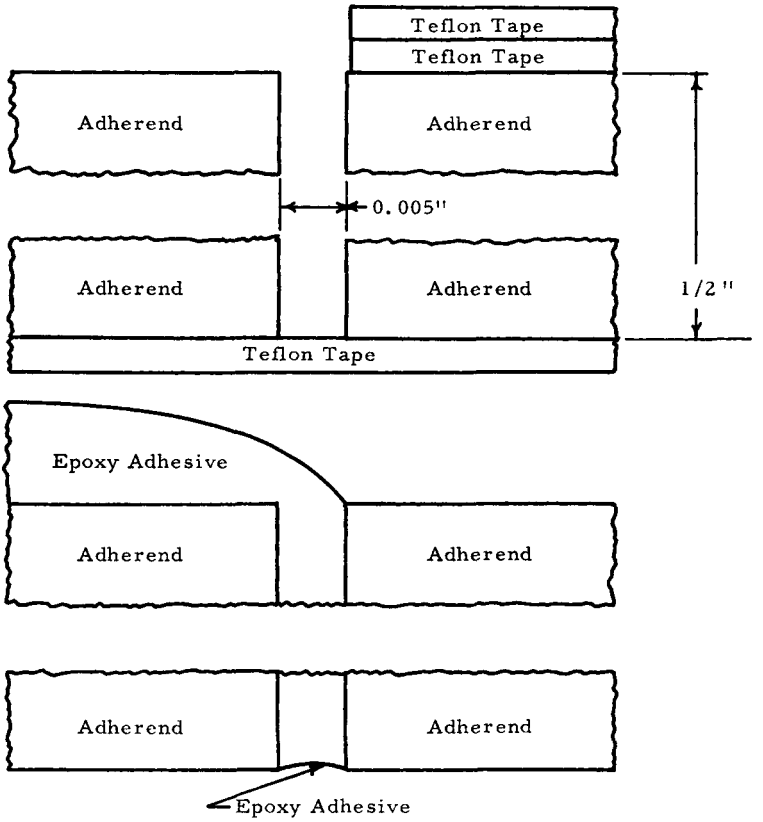

Fig. 4. Schematic of epoxy bond material casting overrun onto adherends, allowing exposure to environment on both sides: (top) as taped prior to casting epoxy adhesive; (bottom) after casting and removal of tape.

by a coding system as A/B, where A is the parts per hundred resin addition of the TEPA hardener to DER 332, and B is the post-cure temperature (Farenheit). For example, 10/180 represents an epoxy containing 10 phr of TEPA which has been post-cured at 180°F. This designation is used throughout this text.

Testing Procedure

All stress corrosion work was carried out on specimens precracked in an increasing load test. A brief description of this test technique (which has been described in detail[1,2]) follows. Post-cured specimens are supported in an Instron tensile machine and loaded in tension through pin grips using the loading holes near the specimen end. Load versus deflection is plotted on an X–Y recorder as a crack is propagated in the adhesive. Test results are converted to fracture toughness values by using the definition of critical strain energy release rate, $\mathcal{G}_c$:

$$\mathcal{G}_c = (P_c^2/2b)\ (\partial C/\partial a) \tag{1a}$$

where P_c is the critical load at onset of rapid fracture (pounds) C, is the specimen compliance, i.e., δ/P(inches per pound), δ is the displacement of load (inches), b is the specimen thickness (inches), and a is the crack length (inches).

In an earlier paper[4] it was shown that by properly contouring the specimen dC/da could be made independent of a. For the selected specimen contour and thickness chosen, $dC/da = 144 \times 10^{-6}$ in.$^{-1}$-lb^{-1})

$$\mathcal{G}_c \text{ (lb/in.)} = 144 \times 10^{-6} \text{ (in.}^{-1}\text{-lb}^{-1}) \; P^2 \text{ (lb.}^2) \tag{1b}$$

Values of strain energy release rate less than $\mathcal{G}_c$ are obtained by applying loads less than P_c. These subcritical loads are designated as P_a, and the corresponding crack extension forces, $\mathcal{G}_a$. When the crack extends at these loads, $\mathcal{G}_a$ becomes $\mathcal{G}(\dot{a})$.

In the previous study, CoB crack velocities were determined after the test involving use of the ripple marking technique described earlier.[1] To determine crack velocities resulting from stress corrosion, two methods were used. For those tests where stress corrosion cracking was allowed to continue for a fixed time, i.e. 100 hr, at a given humidity and applied crack extension force $\mathcal{G}_a$, the amount of crack extension was obtained from fracture appearance. In the case of SCC crack extension, the fracturing occurred at the interface (IF) with its starting point near the end of the center of bond (CoB) increasing load crack. Since the increasing load retest of the specimen after exposure was always fast enough to cause the crack to revert from IF to CoB, the extent of SCC damage was the length of IF fracturing between the two CoB regions. Average crack velocity for this test condition is the total IF length divided by the total test time; for most cases 100 hr.

In those tests where liquid water was used at the crack tip instantaneous velocities at different applied loads were obtained by the use of a displacement gage. Since the compliance change with crack length of the contoured specimen is linear the change in crack length during the test can be obtained directly from changes in displacement; this can be shown as follows:

For the case where P_a is constant,

$$dC/da = (1/P) \; (d\delta/da) \tag{2a}$$

thus

$$d\delta/da = 144 \times 10^{-6} \, P \tag{2b}$$

For example, at an applied $\mathcal{G}_a$ of 0.30 lb/in. and P_a of 45 lb,

$$da = 153 d\delta \tag{3}$$

Thus, a displacement of 10 mils at the loading holes represents a crack length change of 1.53 in.

If we take a time derivative of the expression for a we obtain

$$\dot{a} = 153\dot{\delta} \tag{4}$$

Fig. 5. Constant-humidity static fatigue exposure box. Loading is through take-up nut at top access hole not shown. Air circulation is maintained with a small fan not seen. Constant-humidity solutions are in glass tanks seen under loading weights.

for the particular adherend geometry and load selected. Thus if 10 mils of displacement change were noted during a 2-day exposure interval a crack velocity of 0.53 mil/min would be indicated.

The exposure of adhesive specimens to varying humidities was done in the cabinets shown in Figure 5. These cabinets had a volume of about 13 ft^3 and were provided with timers and microswitches for each of five shock mounted loading trains. Specific relative humidities were obtained with solution tanks appropriate for a particular humidity and a circulating fan. For the highest humidities, water was used in conjunction with a wicking arrangement that exposed up to 700 $in.^2$ to evaporation. Due to temperature inhomogeneities within the cabinet the smallest depression of the dew point observed was 0.5°C corresponding to a relative humidity of 96%. Most of the values of $\dot{a}$ obtained in the humidity cabinet were average values. If the crack did not extend over the full length of the specimen during the 100-hr exposure, the length of the IF crack was measured after the specimen was broken open subsequent to exposure, and the IF crack length divided by 100 hr to obtain $\dot{a}$. The humidity cabinets were equipped with timers for each loading train. For those specimens that fractured completely in less than 100 hr, the IF crack length was divided by the measured exposure time.

For tests with water in direct contact with the specimen, instantaneous rather than average velocities were measured. The precracked specimen was Teflon-taped around the bond line such that a trough was formed to hold the water. It was then placed in a loading train equipped with a dis-displacement gage and loaded to a particular $\mathcal{G}_a$ Once loaded, liquid water was added to the tape trough and the level maintained for the duration of the test. The output of the displacement gage was then recorded on an x–time instrument. Crack velocities determined in this manner were seldom constant due to a number of as yet unidentified causes, e.g., reinitia-

tion of an IF crack from the preexisting CoB increasing load fracture and a variation in the size of an area damaged by advanced separation ahead of the main crack. Thus, the amount of time allotted to a given $\mathcal{G}_a$ for determination of the associated crack velocity $\dot{a}$ was not fixed. Cracks were allowed to grow until $\dot{a}$ was constant over about an hour. Once a rate was established at a specific $\mathcal{G}_a$, the specimen was loaded or unloaded to a new value and the process repeated. In this way, the entire $\mathcal{G}_a$ versus $\dot{a}$ curve was developed, and the limit for negligible propagation, i.e., $\mathcal{G}_{scc}$, was estimated.

Instantaneous values of $\dot{a}$ were also measured in some of the constant humidity tests in order to determine the discrepancies between average and instantaneous velocities.

RESULTS

Influence of Water on $\mathcal{G}_c$

Earlier work on fracture of adhesives was concerned with rapid crack extension under continuously increasing loads. Since water was expected to influence slow crack growth in statically loaded adhesive structures, its influence on both the onset and continued propagation of a rapid crack in the increasing load test was first determined. The effect of water in both the liquid and vapor states is shown by several sets of P–δ curves each made in a different environment, and collected on a single specimen. The influence of the various environments is obtained by loading the specimen to its critical value to evaluate $\mathcal{G}_c$ in an ambient environment, unloading it, changing the environment, reloading to obtain $\mathcal{G}_c$ in the new environment, etc.

The specimen whose P–δ curves are shown in Figure 6 consisted of aluminum adherends bonded with 10/180 adhesive. It was first precracked to slightly more than 2 in. and then tested immediately (curve *1*) to obtain a value of $\mathcal{G}_c$ independent of the action of water. Typical of 10/180 adhesive, the P–δ curve was flat. This extended the crack to beyond three inches, after which it was stored three days at ambient humidity (50% RH) and retested (curve *2*). This storage increased the toughness from its initial value of about $\mathcal{G}_c = 0.30$–0.34 lb/in., but the improvement was localized to the region of the crack tip. After the initial "pop," which showed a typical peaked curve, the crack again extended at the earlier value of $\mathcal{G}_c = 0.31$ lb/in. The specimen, whose crack length was now approximately four inches, was then stored at a high humidity (96%) for 17 hr after which the crack was again extended. This more humid storage increased the toughness even more, to $\mathcal{G}_c = 0.39$ lb/in., and in this case the toughness increase persisted, giving a second pop in the approximately one-half inch of crack motion. Some slight elevation of $\mathcal{G}_c$ for the driven crack is evident even after the pop. After extending the crack to about $5^1/_4$ in. to get beyond the water-affected region, the specimen was again unloaded, and liquid water was introduced into the crack while unloaded, and held for 5

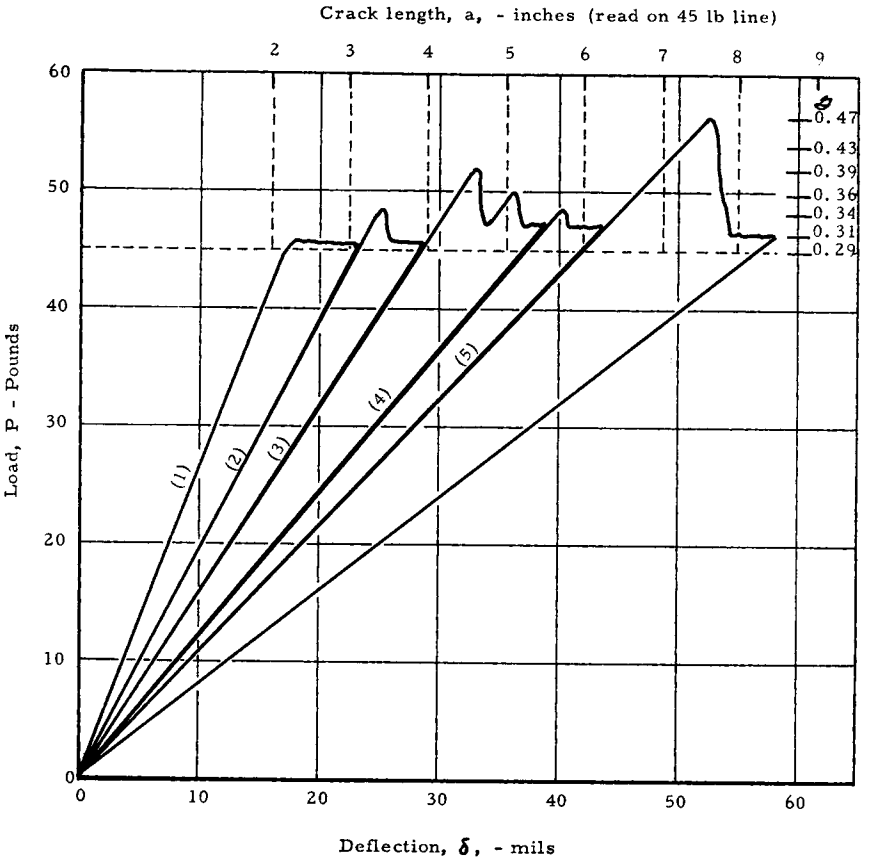

Fig. 6. Increasing load P–δ recording for 10/180 adhesive specimen tested: (*1*) immediately after precracking; (*2*) after 3 day storage in 50% RH; (*3*) after 17 hr storage in 100% RH; (*4*) after introducing water into the crack and storing 5 min; (*5*) same as (*4*) with wetting agent (0.5% Photoflo) added to water. Aluminum adherends, crosshead rate 1.0 in./min.

min. On reloading (curve *4*) a slight increase in toughness was again noted. The crack was now extended to 6 in. and unloaded, water with a wetting agent (Kodak Photoflo) was added to the crack tip, stored 5 min and reloaded (curve *5*). The toughness was now markedly improved to a $\mathcal{G}_c$ = 0.47 lb/in., and again the toughening extended only a small distance beyond the original crack tip.

Attempts were also made to evaluate the influence of water on fracturing under increasing loads for the 12.5/270 adhesive using the same technique described above for the 10/180. Unfortunately, the scatter in toughness within even a single specimen was large enough so that the effect of water in either the liquid or vapor state could not be quantitatively ascertained. Its influence on $\mathcal{G}_c$ was considerably less than it was for the 10/180 adhesive, however, and in no case did the specimens stored in a humid atmosphere, or

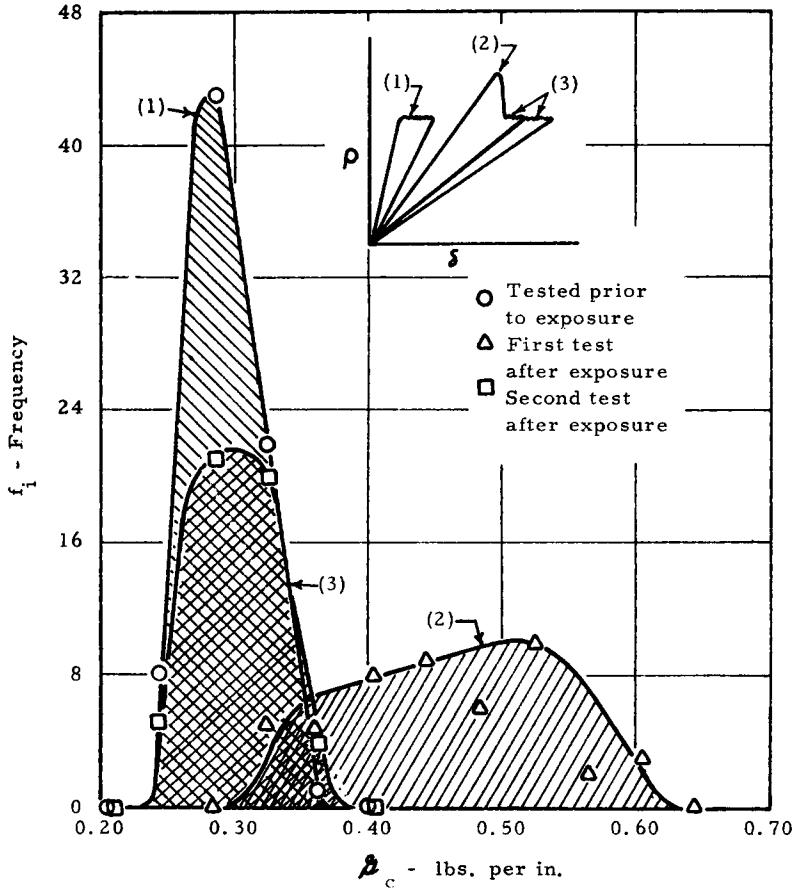

Fig. 7. Distribution of $\mathcal{G}_c$ values for 10/180 adhesive: (*1*) tested prior to exposure; (*2*) first test after exposure; (*3*) second test after exposure. Crosshead rate 1 in./min.

with water in the crack, fall outside the scatter band for $\mathcal{G}_c$ in an ambient atmosphere.

As stated in the Experimental Section, stress corrosion cracking data were obtained by using specimens that were precracked by an increasing load to obtain an initial value of $\mathcal{G}_c$. The precracked specimens were then exposed in a humid atmosphere to evaluate the effect of load on slow crack extension. Specimens that did not completely separate during exposure were then retested to measure $\mathcal{G}_c$ after humid exposure. If the crack at this time were not too long, a second value of $\mathcal{G}_c$ would be obtained on a portion of the adhesive that was well beyond the slowly extended crack. This procedure made it possible to collect statistical data on the fracture toughness of both the 10/180 and 12.5/270 adhesives before and after exposure to water vapor. Post exposure increasing load ($\mathcal{G}_c$) data of two types were obtained; first on a crack whose tip had experienced water vapor exposure under stress, and second, from the crack formed after this first "pop." This second test

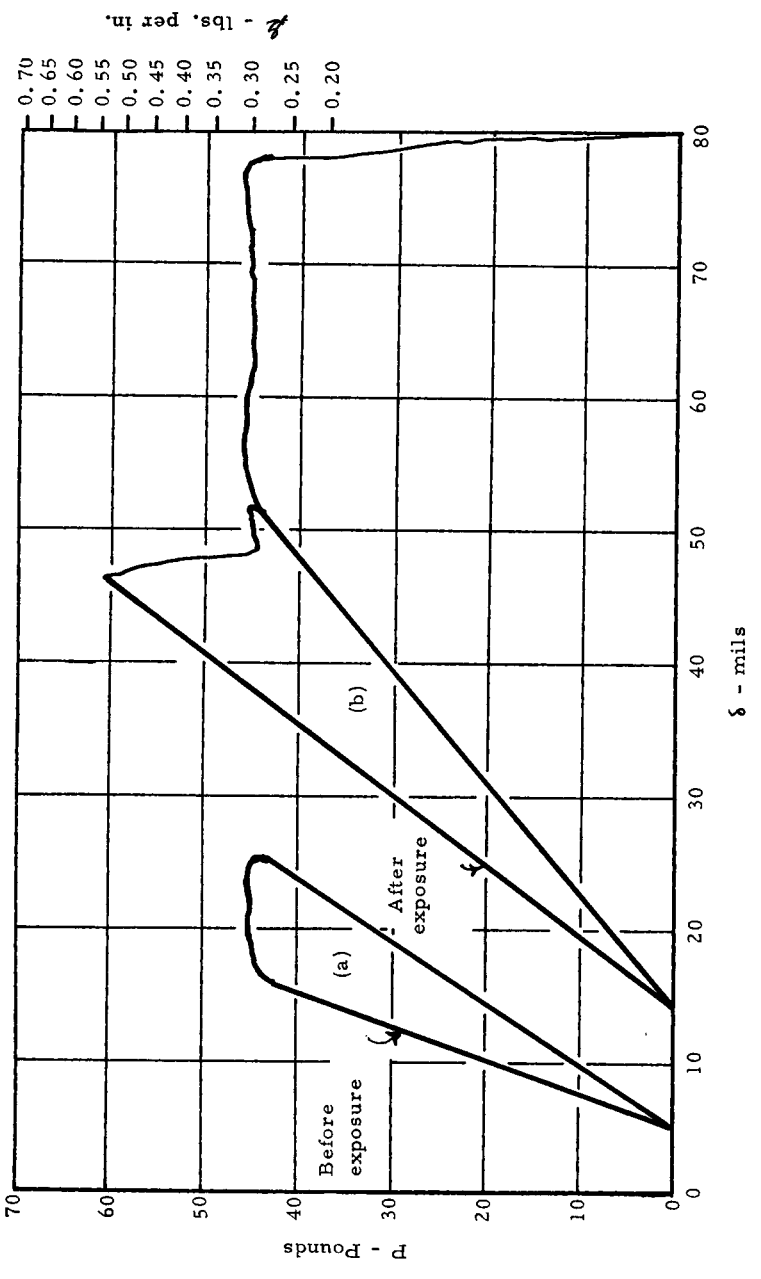

Fig. 8. Load–displacement record of 10/180 adhesive specimen: (*a*) before exposure; (*b*) after exposure at 90% RH.

determined the toughness of a volume of the adhesive that was exposed to water vapor in the absence of a crack.

A plot of these data are shown in Figure 7 for the 10/180 adhesive. The scatter in $\mathcal{G}_c$, prior to exposure is seen to be minimal. Variation in any one specimen is less than ± 0.02 lb/in., and for more than 30 specimens tested in this series, the average toughness was found to be 0.29 lb/in. with a 3σ value of 0.079 lb/in.

Toughness values from the first test after exposure were a great deal more variable. These ranged from 0.31 to 0.64 lb/in. with the peak of the distribution curve occurring at 0.52 lb/in. Toughnesses were always higher than the preexposure $\mathcal{G}_c$ values for any single specimen. The higher $\mathcal{G}_c$ values which occurred after high humidity exposure are consistent with the increased toughness shown by the curves in Figure 6 in which this same material was exposed to the high humidity in an unstressed condition.

The inability of water to produce a toughness increase at significant distances beyond the original crack tip, as shown in Figure 6 for unstressed exposure, was also found for specimens exposed to water while under load. Note in Figure 7 that a second test after stressed exposure resulted in a distribution of toughness values that was identical with the one obtained prior to exposure.

The flat P–δ curve associated with 10/180 adhesive tested in an ambient humidity switched to a peaked curve after unstressed exposure in a high humidity (see Fig. 6). This same change in the P–δ behavior was also found after exposure to a high humidity in the presence of a stress (Fig. 8).

Even though the influence of liquid water and high humidity on $\mathcal{G}_c$ could not be evaluated in single specimens of the 12.5/270 adhesive because of the large scatter in toughness, data similar to those shown in Figure 7 could be collected on the specimens subjected to stress corrosion. As shown by the statistical plot in Figure 9, the toughness of the 12.5/270 adhesive was far greater than that of the 10/180 and the scatter in initiation values was also higher. Initiation values of toughness showed a peak at $\mathcal{G}_c = 0.59$ lb/in., and the 3σ limits were 0.34 lb/in. In addition, the scatter in any one specimen could, at times, equal the scatter range shown by the group. The values of $\mathcal{G}_c$ obtained after exposure are essentially the same as those obtained prior to exposure and exhibited about the same scatter except for a few points which were beyond the range of the abscissa in Figure 9. Scatter in this tougher adhesive seems to be related to slight variations in crack velocity at instability (see Fig. 1). Once $\mathcal{G}_a$ equals $\mathcal{G}_c$ for the stationary crack, the crack jumps, outrunning the crosshead displacement rate (by up to several orders of magnitude) and arrests at about an inch from the initiation point, generating a peaked P–δ curve typified by the one shown in Figure 3*b*. Arrest occurs because the slow moving cross-head cannot maintain the load necessary to keep the crack running. Thus the load decreases to the value of $\mathcal{G}_c$ for crack arrest. The jump length then represents the cracking distance necessary to reduce the load P to the value associated with crack arrest.

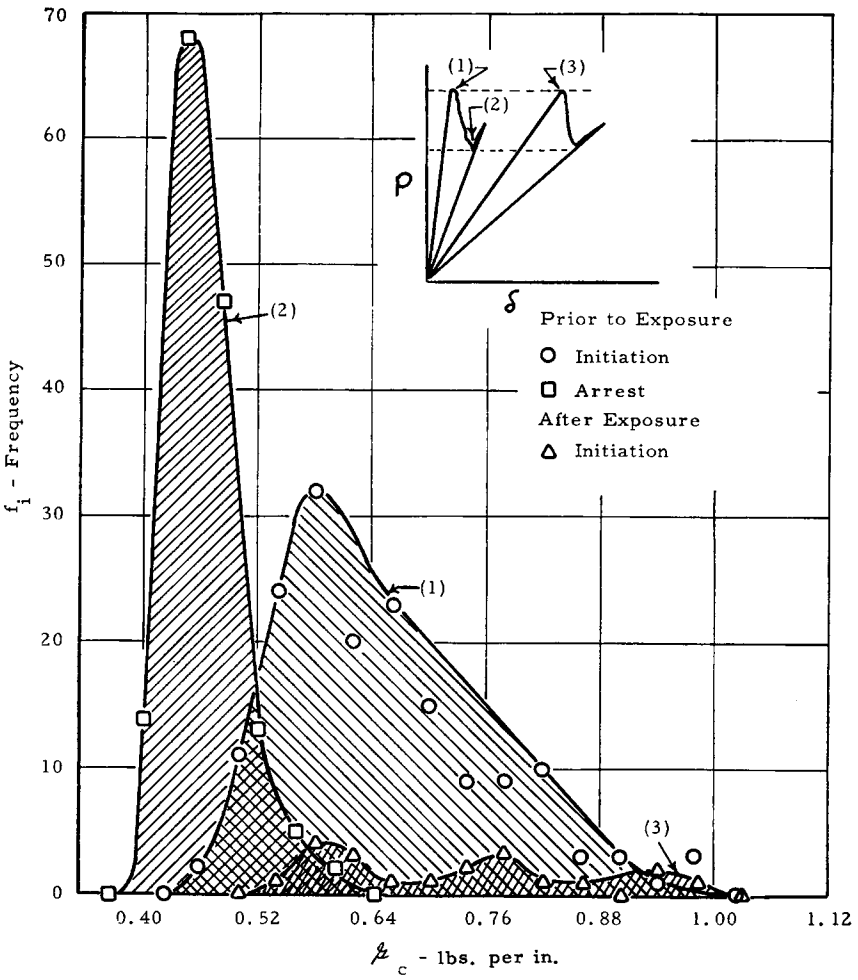

Fig. 9. Distribution of $\mathcal{G}_c$ values for 12.5/270 adhesive tested: (*1*) prior to exposure, initiation; (*2*) prior to exposure, arrest; (*3*) after exposure, initiation. Crosshead rate 1 in./min.

The plot of arrest toughnesses in Figure 9 is seen to exhibit far less scatter than the initiation value of $\mathcal{G}_c$. Even though the arrest value for 12.5/270 adhesive is much lower than its initiation value, i.e., 0.47 lb/in., it is still considerably higher than initiation or arrest for the 10/180 adhesive. The 3σ limit for arrest was 0.11 lb/in.

Stress Corrosion Cracking (scc)

Crack Morphology. The most striking difference between fracturing under increasing load, and stress corrosion cracking was the crack morphology. As stated in an earlier section, cracks for the stress corrosion study were always initiated by increasing load tests to obtain a value of $\mathcal{G}_c$ for the

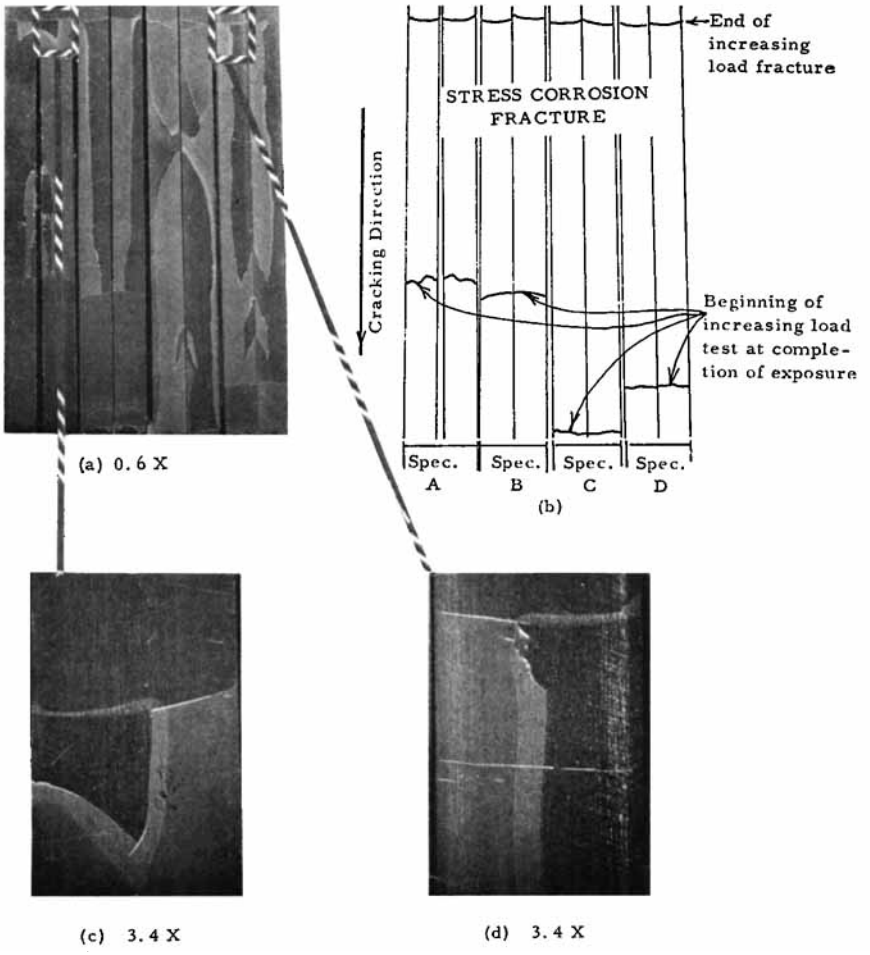

Fig. 10. Fracture surface photographs and schematics after 100 hr exposure at 96% RH: (*a*) four specimens showing various crack extensions lengths during test (low magnification); (*b*) schematic drawing of (*a*); (*c*) increased magnification of one specimen in (*a*) showing epoxy separation; (*d*) same as (*c*), showing double debonding from both sides. Aluminum adherends, 10/180 adhesive.

test specimen, and for both adhesive systems such cracks always occurred at the center of the bond (CoB). During exposure at values of $\mathcal{G}_a$ appreciably less than $\mathcal{G}_c$, at humidities above a few per cent, the crack extended near one or another interface. The start of the stress corrosion interface crack is not continuous with the former CoB crack but starts at the air–adherend–adhesive edges in the region of the CoB crack tip. These interface (IF) cracks propagate inward from the edges until they reach the other edge or the stress field of the second crack propagating from the opposite edge. If the IF cracks growing from the two edges do not lie on the same plane (e.g., one lies "above" the adhesive layer and one "below") there may be propagation of both towards the opposite edges as well as in the length

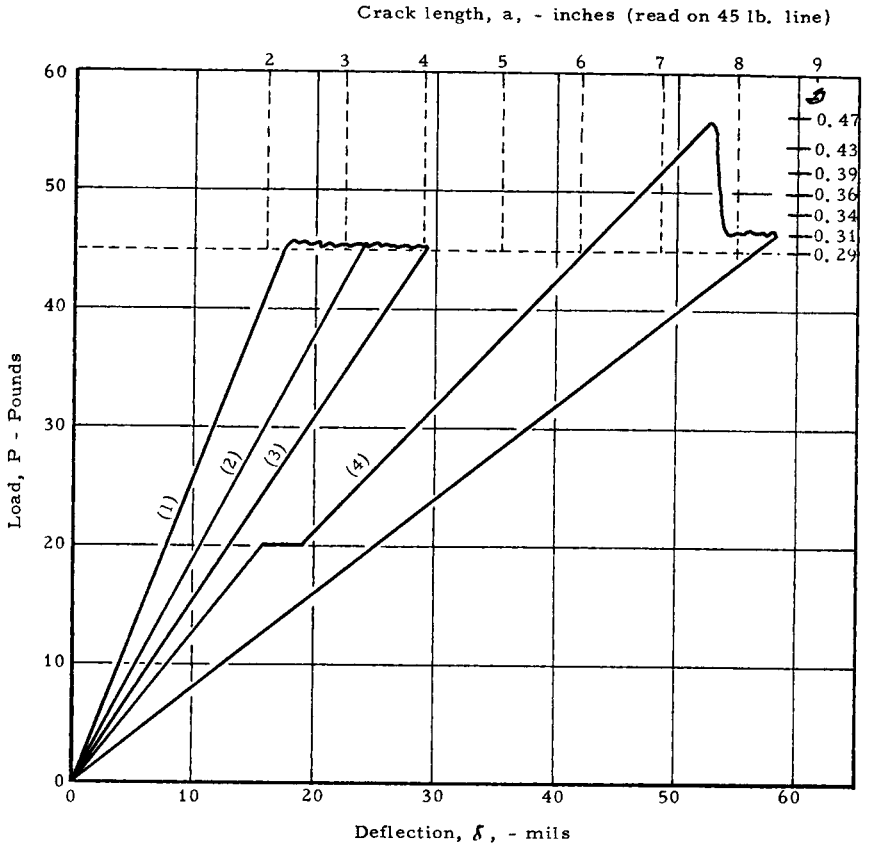

Fig. 11. Increasing load P–δ recording for 10/180 adhesive specimen tested before and after 100 hr exposure to a high $\mathcal{G}_a$: (*1*) tested immediately after precracking; (*2*) retested; (*3*) unloaded for exposure; (*4*) retested after exposure. Note step in curve *4*. Aluminum adherends, 10/180 adhesive.

direction even after they have arrived at the same region of the adhesive causing double debonding on a narrow strip over a long length of the specimen (Figs. 10*a*, 10*d*). The tendency for double debonding increases with increasing humidity, and indeed is the feature that distinguishes exposure at high humidity levels. The photographs of Fig. 10 show double debonding over extensive areas characteristic of high humidity (96 percent R. H.) and moderate $\mathcal{G}(\dot{a})$ levels.

Double debonding, near the specimen edges, occurred only on the side of a specimen on which there is no epoxy overrun (see Fig. 4). This inability of water to penetrate the edge of the adherend–adhesive interface which is covered indicates that the diffusion of water even through thin layers of epoxy and through a well bonded interface not subject to direct tension requires an appreciable amount of time. It was noted that while double debonded areas could be easily stripped of adhesive mechanically, the re-

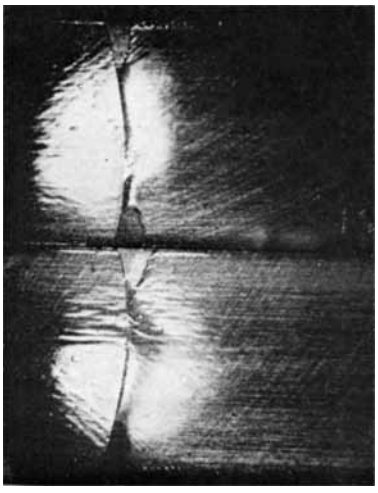

(a) 3.7 X

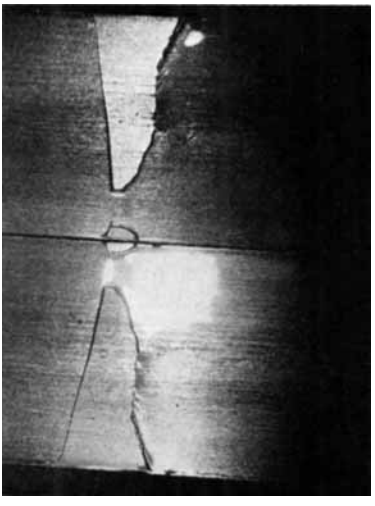

(b) 3.7 X

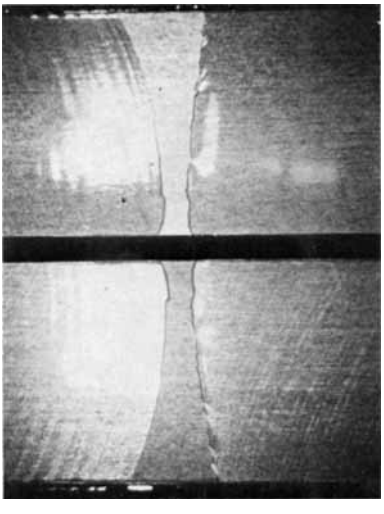

(c) 3.7 X

Fig. 12. Fracture surface photographs of specimens exposed to 100 hr exposure at 58% RH and a low $\mathcal{G}_a$: (*a*), (*b*), (*c*) arranged in order of increasing exposure $\mathcal{G}_a$ level. Aluminum adherends, 10/180 adhesive.

maining adhesive just beyond the debonded area was tenaciously bonded to one or the other adherend.

At the completion of exposure, the crack always reverted to the CoB on subsequent increasing load testing as shown for the specimens in Figure 10*a*. Both the fracture appearance and the shape of some of the P–δ curves indicate that the initial CoB fracture and the IF fracture formed during static exposures are not continuous. For example, in the photo-

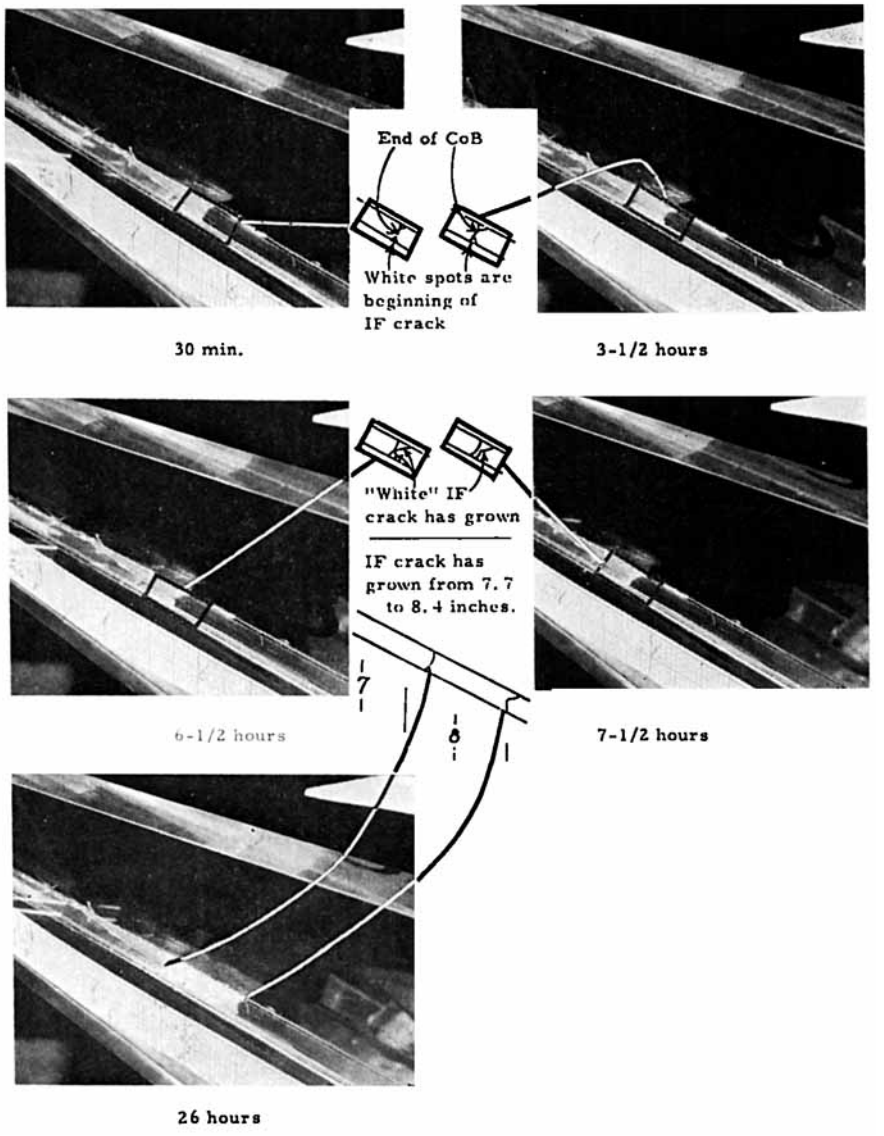

Fig. 13. Stress corrosion cracking photographed through glass adherends (58% RH).

graphs of Figure 10*a* and in the two enlargements, (*c* and *d*,) it can be seen that the interface fracture extends backward some slight amount under the initial CoB fracture. For this to occur there must have been a connecting, load carrying ligament between the CoB and IF fracture surfaces. Further evidence of this discontinuous cracking is seen by the shape of the P–δ diagrams. In a number of these, especially when the IF crack length is small, the loading portion of the elastic curve has a slight step as shown in the recording number 4 in Figure 11. The specimen compliance up to

the step has only a slightly different value than it had prior to exposure; after the discontinuity, the compliance value changes to that for the larger crack length including the IF fracture. This suggests that the connecting ligament between the original CoB and IF fracture requires some appreciable load to fracture.

Two types of tests verified the fact that the stress corrosion cracks reinitiate at the air–adhesive–adherend interface, and grow concurrently

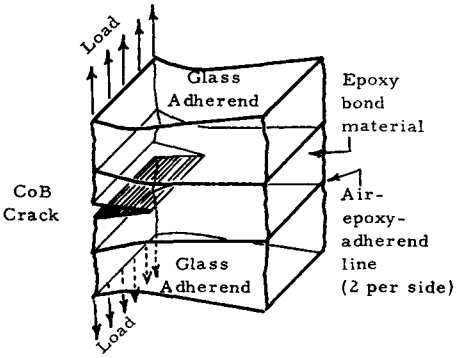

(a) Section of tapered glass adherends adhesive specimen with increasing load CoB fracture prior to stress corrosion exposure.

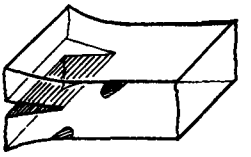

(b) Bond section only showing two static fatigue cracks both formed at lower interface-air boundary and propagating toward one another. (These cracks may be formed on opposite interfaces on occasion.)

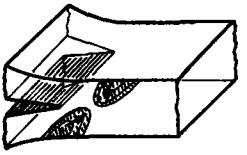

(c) Successive stages of crack extension before link up.

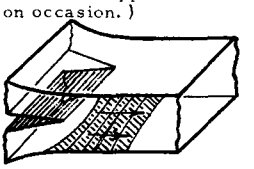

(d) Link up of interface crack and successive propagation. Note that end of CoB crack does not link up with interface crack. (Start of interface crack may occur slightly behind CoB crack.)

Fig. 14. Schematic drawing of stress corrosion crack extension.

across the specimen thickness and along its length. The first of these test series used aluminum adherends and 10/180 adhesive. The specimens were first precracked by an increasing load to form CoB cracks. These were then stress corrosion cracked in 58% RH, at a value of $\mathcal{G}_a$ that was low enough to cause only slight crack extension at the interface within the time of the exposure, after which the specimens were subjected to an increasing load to form a second CoB crack. The fracture appearance of three such specimens arranged in order of increasing $\mathcal{G}_a$ are shown in Fig. 12. The IF

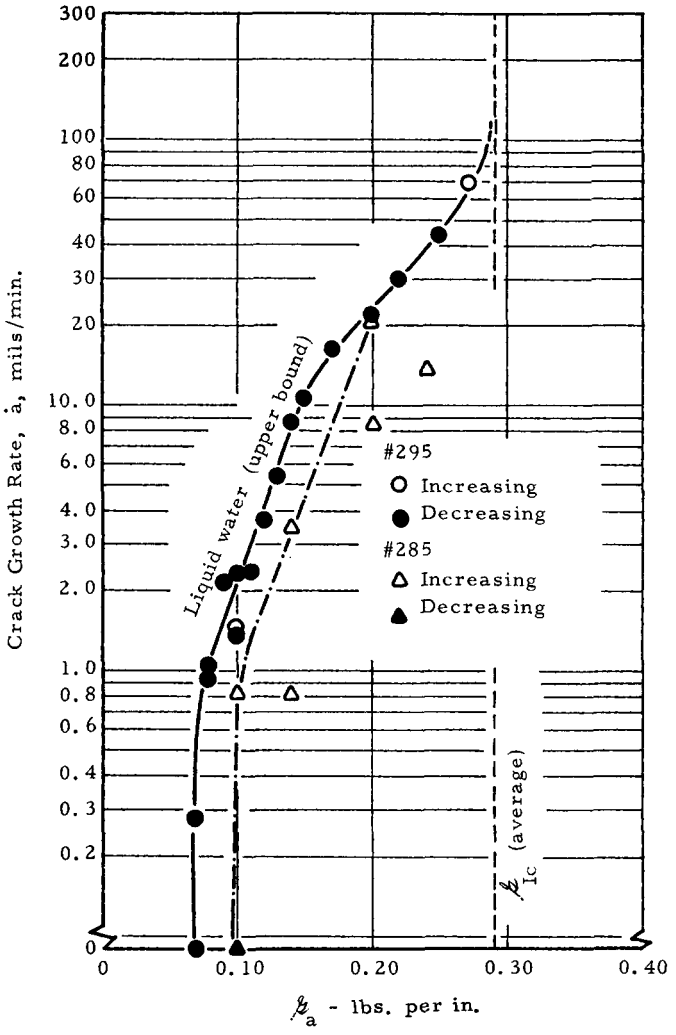

Fig. 15. Stress corrosion of 10/180 adhesive in liquid water. Note that $\mathcal{G}_{see} \cong 0.08$ lb/in.

fractures are seen to start at the specimen edges and grow across the specimen width and then along its length to form the final separation.

In another series of tests, glass adherends were used so that the fracture surface could be observed directly. A series of photographs of successive stages of cracking in such a specimen is shown in Figure 13. Again, the crack propagation was found to occur by debonding at the interfaces and by subsequent movement of the separation along the length of the specimen. Lapsed time movies were also made of stress corrosion cracking in a number of other glass–adhesive specimens, and crack extension was found to be quite nonuniform. Although some cracks advanced at about a con-

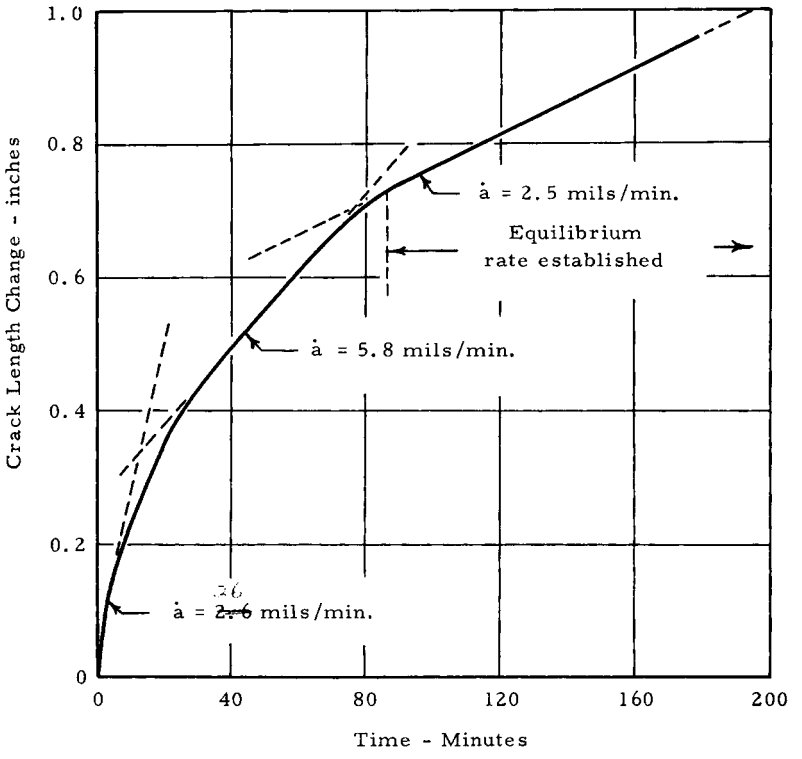

Fig. 16. Typical crack extension record obtained on 12.5/270 adhesive specimen exposed to liquid water.

stant velocity across the complete specimen thickness, in other cases, extension was by the formation of a series of fingers, with the crack wandering between the top and bottom interfaces as it progressed, implying that considerable scatter might be expected in stress corrosion cracking data.

An idealized representation of initiation and extension of a stress corrosion crack is shown in Figure 14.

Stress Corrosion Cracking Rates. Slow crack extension rates were studied with both liquid water and in a humid environment. As pointed out in the Experimental Section, two methods were used to evaluate cracking rate $\dot{a}$. Since slow cracking is stable, instantaneous values of $\dot{a}$ can be determined by monitoring $\dot{\delta}$ [see eq. (5)]. Where this method is not convenient, a static load can be applied to the specimens for some arbitrary time, e.g., 100 hr, and an average rate ascertained by examining the specimen at the completion of the exposure.

The tests in liquid water were carried out in an ambient environment, and required almost no preconditioning. For this exposure condition it was most convenient to evaluate instantaneous rates since the applied loads on a given specimen could be changed after the crack ran a short distance, and in this way collect a large number of points on a single specimen. So

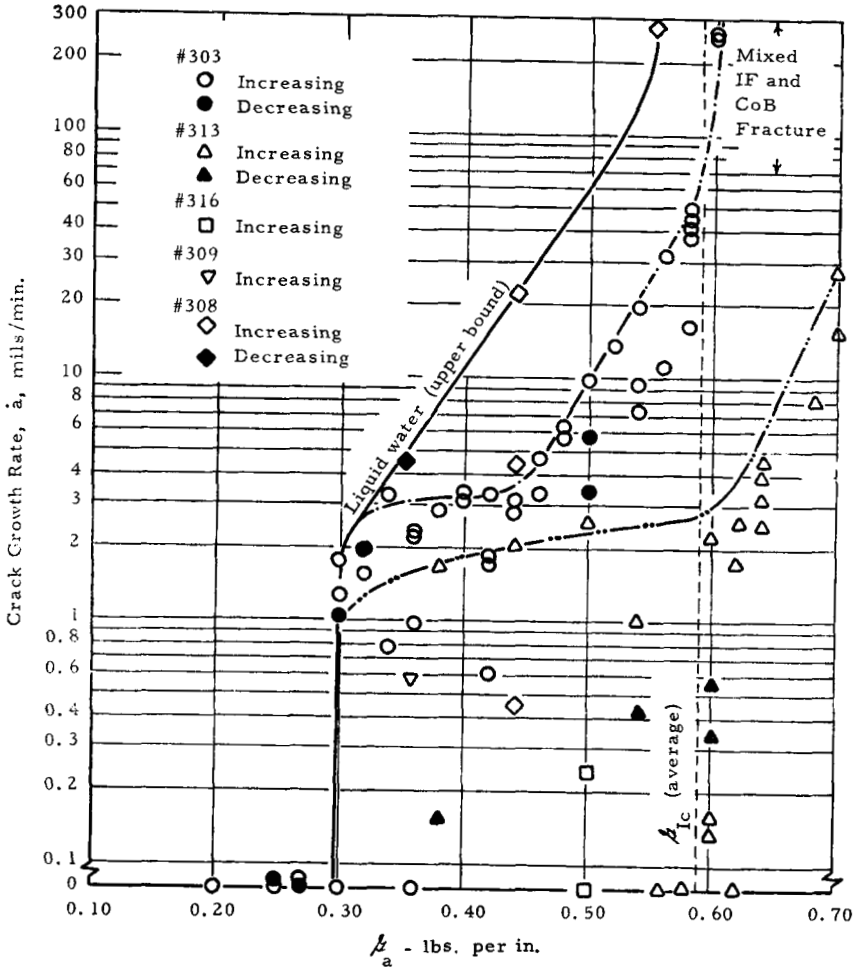

Fig. 17. Stress corrosion cracking of 12.5/270 adhesive in liquid water. Note that $\mathcal{G}_{scc} \cong 0.30$ lb/in.

long as the instantaneous $\dot{a}$ was an equilibrium value it was expected to be the same as the average value of $\dot{a}$. This method was not as economical for collecting data on the effect of humidity since the constant humidity boxes had to be conditioned for the order of a day prior to loading the specimen. Once the specimen was conditioned and loaded, it seemed advisable to run long cracks, and use average values of $\dot{a}$, in order to minimize scatter.

Instantaneous values of $\dot{a}$ obtained on two specimens with liquid water at the crack tip are plotted as a function of $\mathcal{G}(\dot{a})$ in Figure 15 for the 10/180 adhesive. All of these data were collected by establishing a value of $\dot{a}$ at a specific $\mathcal{G}_a$, decreasing or increasing P to change $\mathcal{G}_a$, determining a new $\dot{a}$, etc. The $\mathcal{G}(\dot{a})$ values were both increased and decreased in steps

in order to be certain that there was no effect of the previous load. These are plotted as open or closed symbols, and show that the results are not dependent on whether the load is increasing or decreasing.

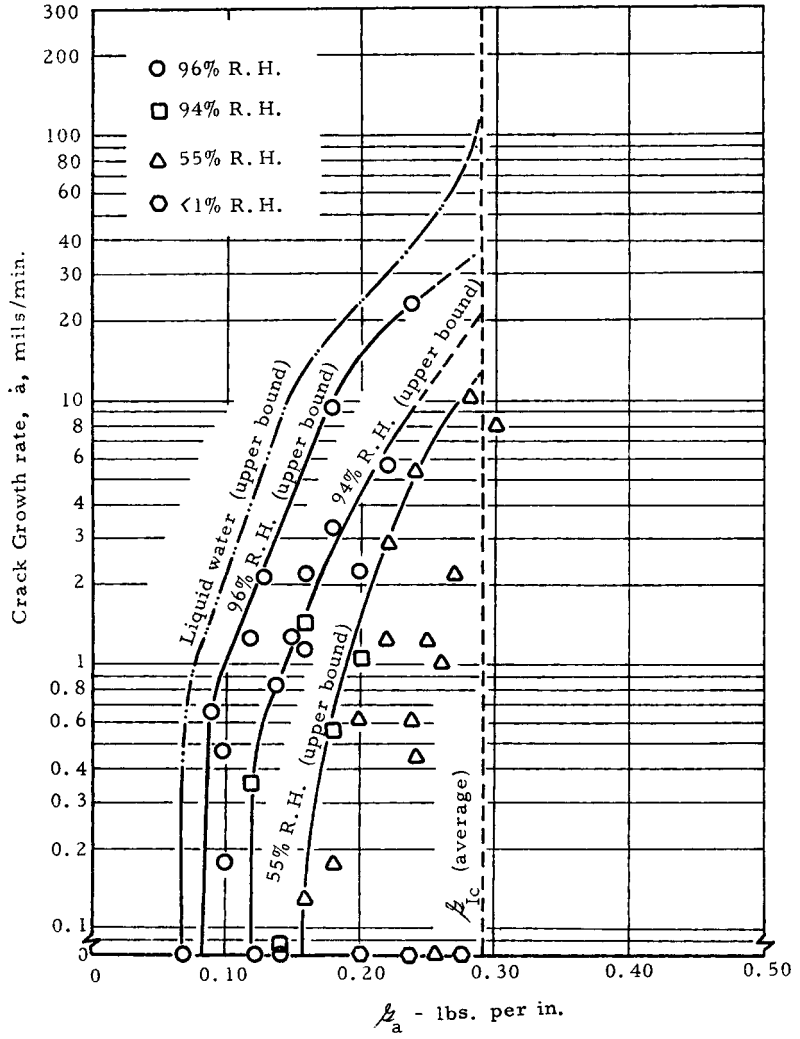

Fig. 18. Stress corrosion cracking of 10/180 adhesive as a function of relative humidity. Note that at the highest humidity $\mathcal{G}_{scc} \cong 0.08$ lb/in., which is similar to the value of $\mathcal{G}_{scc}$ obtained in liquid water (Fig. 15).

In most cases, $\dot{a}$ is not a constant over the interval in which $\mathcal{G}(\dot{a})$ is constant, as shown in Figure 16. Hence, to obtain each point, the cracking rate is monitored at constant $\mathcal{G}(\dot{a})$ until an equilibrium rate is obtained. It is the final value of $\dot{a}$ that is plotted in Figure 15.

In the plot of Figure 15, the upper range of environment controlled

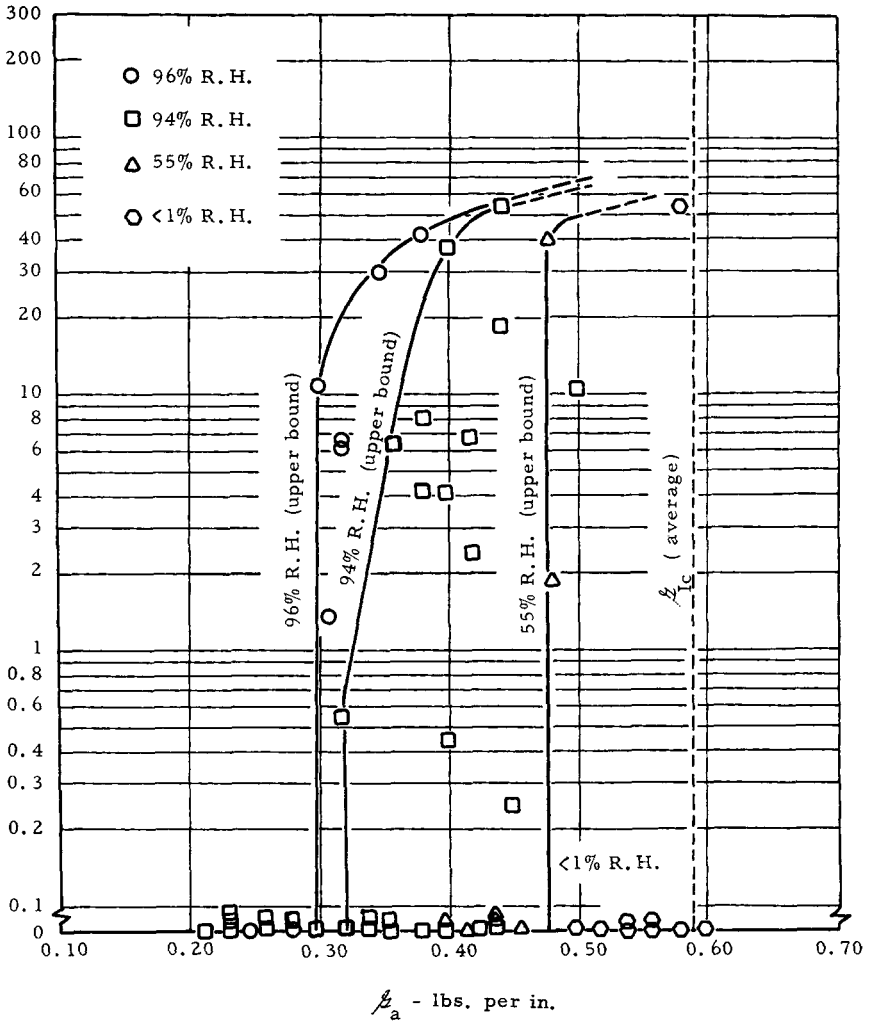

Fig. 19. Stress corrosion cracking of 12.5/270 adhesive as a function of relative humidity. Note $\mathcal{G}_{scc} = 0.30$ lb/in., i.e., the same as for liquid water.

crack extension rates were chosen to characterize the effect of water since this represents the "worst possible" case.

The data suggest that there is a value of $\mathcal{G}\dot{a}$, i.e., $\mathcal{G}_{scc}$, below which the crack cannot extend. For distilled water, and the 10/180 adhesive, $\mathcal{G}_{scc}$ is slightly less than 0.10 lb/in.

Similar tests were also carried out on 12.5/270 adhesive with the use of water at the crack tip (Fig. 17). $\mathcal{G}_{scc}$ for this adhesive is approximately 0.30 lb/in. The ratio of $\mathcal{G}_{scc}$ to $\mathcal{G}_c$ for the 12.5/270 adhesive is about 0.5 while for the 10/180 it is about 0.3. Obviously, the latter is far more sensitive to water than the former.

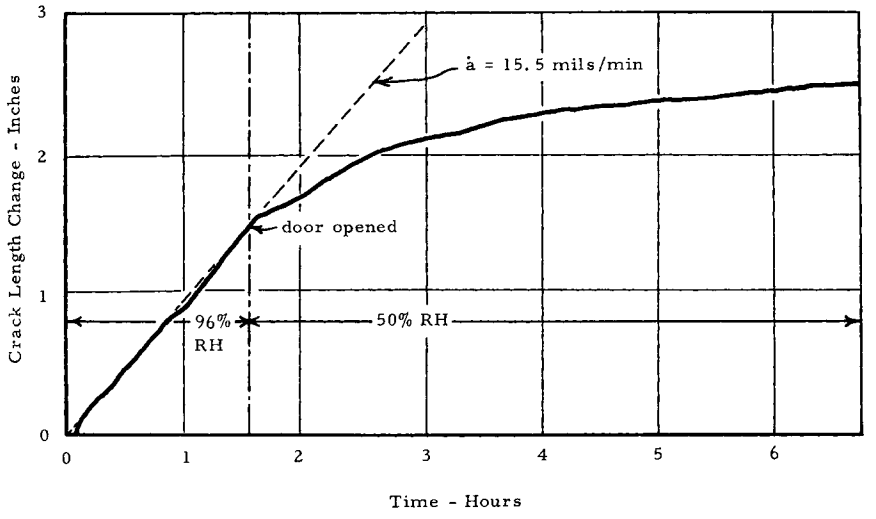

Fig. 20. Stress corrosion cracking of a 12.5/270 adhesive specimen exposed to 96% RH and 50% RH at $\mathcal{G}_a = 0.32$ lb/in.

Even though both adhesives exhibited reasonably well defined $\mathcal{G}_{scc}$ values, the scatter in propagation rates was quite different: the 10/180 adhesive showing far less scatter than the 12.5/270.

For both adhesive systems, tests were also made in relative humidities of 96, 94, or 90, 55, and <1% RH. The data obtained are average values based on 100 hr of exposure. Since a typical useable crack length of a specimen is 5–10 in., values of $\dot{a}$ less than 1–2 mil/min would not cause complete separation while rates in excess of this would, within the time limit of the exposure. For the cracking rates that caused complete separation, the exposure time to fracture, obtained from an interval timer, was divided by the IF crack length to obtain $\dot{a}$. Since the last inch or so of crack extension occurred in a portion of the specimen in which $\mathcal{G}_a$ increased rapidly with a, for constant load, this part of the specimen is marked by reversion to CoB fracture.

Average $\dot{a}$ versus $\mathcal{G}(\dot{a})$ curves for the 10/180 and 12.5/270 adhesive are shown in Figures 18 and 19. Again, as in Figures 15 and 17, the curves in these charts represent upper bound values, i.e. the envelope of fastest cracking at the specific humidity. The scatter in these curves, particularly for the 12.5/270, is quite broad, nevertheless two characteristics of cracking are apparent. First, the value of $\mathcal{G}_{scc}$ and $\dot{a}$ at constant $\mathcal{G}_a$ are functions of the humidity, and for the highest humidity (96% RH) $\mathcal{G}_{scc}$ is the same as the value obtained with distilled liquid water. Second, if the humidity were kept low enough, no stress corrosion crack growth was observed.

The influence of humidity on cracking rate can be dramatically demonstrated on a single specimen by changing the humidity at constant $\mathcal{G}_a$. The 12.5/270 adhesive exhibited SCC at $\mathcal{G}_a = 0.32$ lb/in. in 96% RH, but

not at 50% RH (Fig. 19). A specimen made with this adhesive was loaded to $\mathcal{G}_a$ = 0.32 lb/in. and allowed to crack in a 96% RH environment for some time, after which the door of the constant humidity cabinet was opened, exposing the specimen to ambient humidity (approximately 55% RH). As shown in Figure 20, the cracking rate decreased as soon as the door was opened, and as the specimen dried up, cracking stopped.

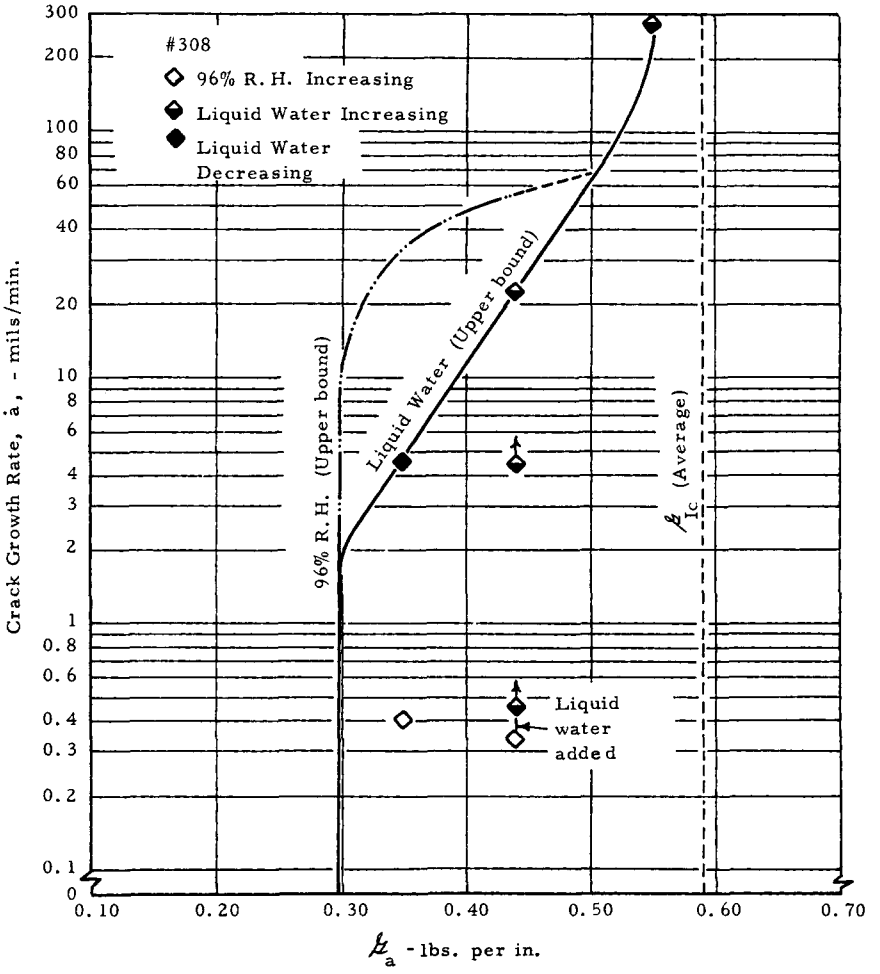

Fig. 21. Comparison of crack growth rates in a high humidity environment and liquid water for 12.5/270 adhesive.

The rate data collected on 10/180 with liquid water and 96% RH are almost identical; indeed the water data collected on two specimens bracket the upper bound value for 96% RH. For the 12.5/270 adhesive, liquid water would appear to be less damaging than the highest humidity even though $\mathcal{G}_{scc}$ is the same for both environments.

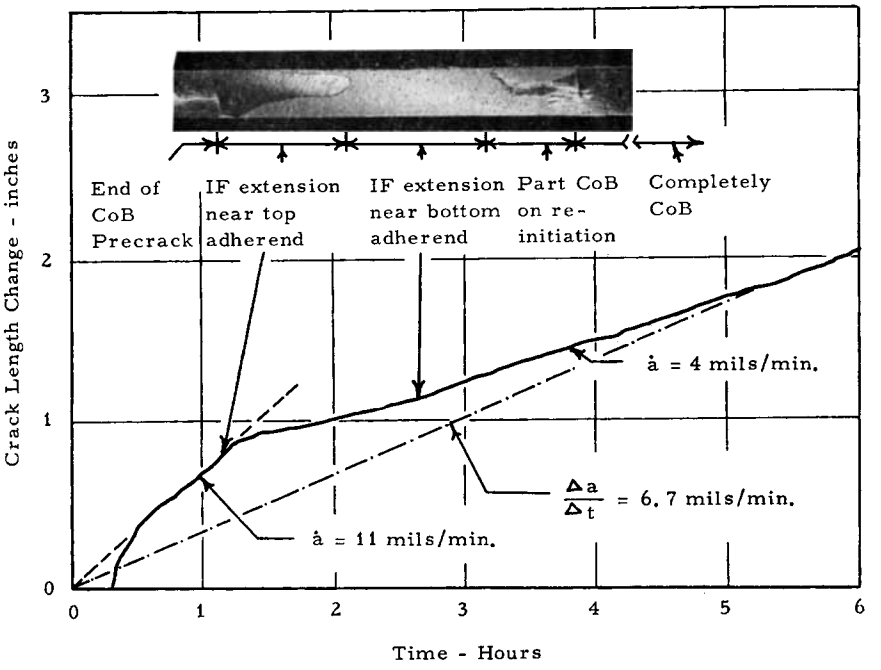

Fig. 22. Stress corrosion cracking of 12.5/270 adhesive specimen exposed to 96% RH at $\mathcal{G}_a$ = 0.32 lb/in, if areas on curve are connected to corresponding areas on specimen fracture surface photograph.

In order to ascertain whether water was less damaging than a high humidity or whether the difference was due to material scatter, a single specimen was alternately loaded in 96% RH and in water. As shown by the data collected on specimen 308 (Fig. 21), it does not seem likely that 12.5/270 adhesive is less damaged by liquid water than by a high humidity.

All of the data shown in Figures 15, 17, 18, and 19 represent stable crack extension with interface cracking. If the applied load is sufficiently high, the interface separation will begin to occur from the outside edges of the specimen. Due to this separation the effective thickness of the specimen is now reduced so that $\mathcal{G}_a$ applied to the uncracked ligament might exceed $\mathcal{G}_c$. In such a case, the crack will extend IF on its outside edges and CoB in the center. Such mixed crack extension was rare in the 10/180 adhesive, but occurred in almost all of the 12.5/270 adhesive specimens where $\dot{a}$ exceeded 80 mils per minute.

The large scatter in cracking rates for the 12.5/270 adhesive, as compared with the 10/180, can be attributed at least in part to the poorly defined shape of the crack tip. In increasing load testing both adhesives form slightly curved crack fronts so that the cord length of the element separating the cracked and uncracked material is approximately equal to the specimen thickness, b. For the 12.5/270 adhesive subjected to SCC, long fingers of interface cracking extend out beyond the position of the

"average" crack front location. This continuously changing cord length causes an under- or overestimation of $\dot{a}$ for any particular $\mathcal{G}(\dot{a})$ This dependence of $\dot{a}$ on crack front shape is apparent in Figure 22. The initial change from CoB to IF occurred with a very striking change in crack front shape resulting in a varying propagation rate.

DISCUSSION AND CONCLUSIONS

Effect of Water on Increasing Load Behavior

An earlier report by the authors has shown that epoxy hardened with a room temperature curing amine hardener displayed two types of fracture behavior in the presence of a continuously increasing load. With low post-cure temperatures, crack extension occurred at a rate dictated by the machine cross-head displacement rate. Such materials, (e.g. 10/180) show identical initiation and arrest toughnesses. For the system where higher post-cure temperatures are used (e.g., 12.5/270) the initiation toughness is considerably higher than its arrest value.

For the 10/180 adhesive, either storage in a high humidity or the introduction of liquid water to the crack tip causes a marked increase in fracture initiation toughness (for CoB failures) but no change in the arrest value. The influence of water exists only in the immediate region of the crack tip implying that the action of water at the crack tip is slow and cannot follow cracks extending at rates of $\dot{a} = 2$ ft/sec.

For the 12.5/270 material, on the other hand, neither high humidity storage nor liquid water at the crack tip had a pronounced effect. Neither of these environments were able to cause a displacement of toughness values from the rather broad scatter band exhibited by this material tested without preconditioning.

Stress Corrosion Cracking

While rapid cracking for the two epoxy formulations studied invariably occurs at the center of the bond, slow crack extension in a humid environment or liquid water always occurs at the interface. Stress corrosion cracking requires that the corroding medium be available in a region of high stress. Hence slow cracking always starts in the region of the CoB crack tip (where the stresses are highest) at the air (or water) exposed portion of the adherend–adhesive interface. If vapor or liquid water is excluded from this location, cracking at less than $\mathcal{G}_c$ does not occur. The fact that the water is unable to penetrate the two mil thickness of adhesive separating the CoB fracture surface and the interface suggest that the rate at which water can diffuse through epoxy is limited.

The reaction of the joint to water at the center and interface of the bond are exactly opposite: water either toughens or does not affect the adhesive at the CoB crack tip while lowering the load carrying capability at the interface. Hence, if it were possible to protect the interface from water while

allowing it to enter CoB cracks, wet joints in glass reinforced plastics would be as tough as, or tougher than dry ones.

In the presence of water, cracking is always a rate dependent competition between a potential crack extension at the center of the bond and interface locations. The critical cracking rate for this epoxy system is approximately $\dot{a} = 0.05$ f/sec. Below this rate, cracking occurs at the water damaged interface, and above this value in the center-of-bond.

There is a value of $\mathcal{G}_a$, i.e., $\mathcal{G}_{scc}$, below which slow cracking will not occur. $\mathcal{G}_{scc}$ was found to decrease as the relative humidity was increased. For a high humidity (96% RH) and liquid water, $\mathcal{G}_{scc}$ had the same value.

The adhesive that was less sensitive to water in increasing load testing (12.5/270) was also less damaged by water in stress corrosion cracking. The ratio of $\mathcal{G}_{scc}/\mathcal{G}_c$ for the 12.5/270 was approximately 0.5 while it was only 0.3 for the 10/180 adhesive.

References

1. S. Mostovoy and E. J. Ripling, *J. Appl. Polym. Sci.*, **10**, 1351 (1966).
2. E. J. Ripling, S. Mostovoy, and R. L. Patrick, *Materials Res. Stand.* No. 3, **64**, 129 (1964).
3. E. J. Ripling, S. Mostovoy, and R. L. Patrick, *ASTM Spec. Tech. Publ.* **No. 360**, 5 (1963).
4. S. Mostovoy, P. B. Crosley, and E. J. Ripling, *Materials*, **2**, No. 3, 661 (1967).

Received September 5, 1968